Binary X-ray sources of Be-type: studying accretion extremes with the X-ray telescope XMM-Newton

Nicola La Palombara[1]

L. Sidoli[1], S. Mereghetti[1], G.L. Israel[2], P. Esposito[3,1]

[1]INAF - IASF Milano, [2]INAF – OA Roma, [3]IUSS Pavia

LXVI Congresso SAIt
3 Giugno 2025
Firenze

INAF

- Systems composed of a neutron star (NS) orbiting a Be-type, fast rotating, massive star with a circumstellar decretion disk
- **Two types of BeXRBs** based on orbital characteristics and accretion behavior onto the NS (producing X-rays)

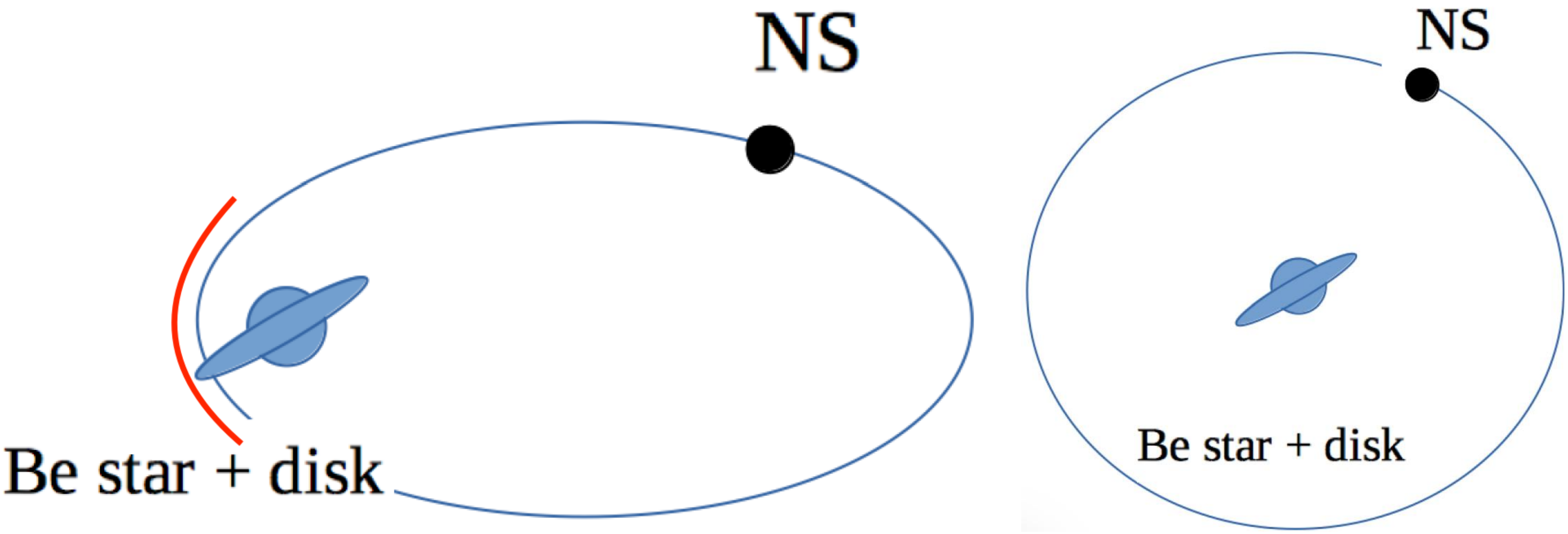

Transient BeXRBs: eccentric orbit
⇓
periodic outbursts near periastron

Persistent BeXRBs: circular orbit
⇓
steady accretion from Be polar wind

XMM-Newton

ESA's flagship X-ray observatory, launched on 10 December 1999

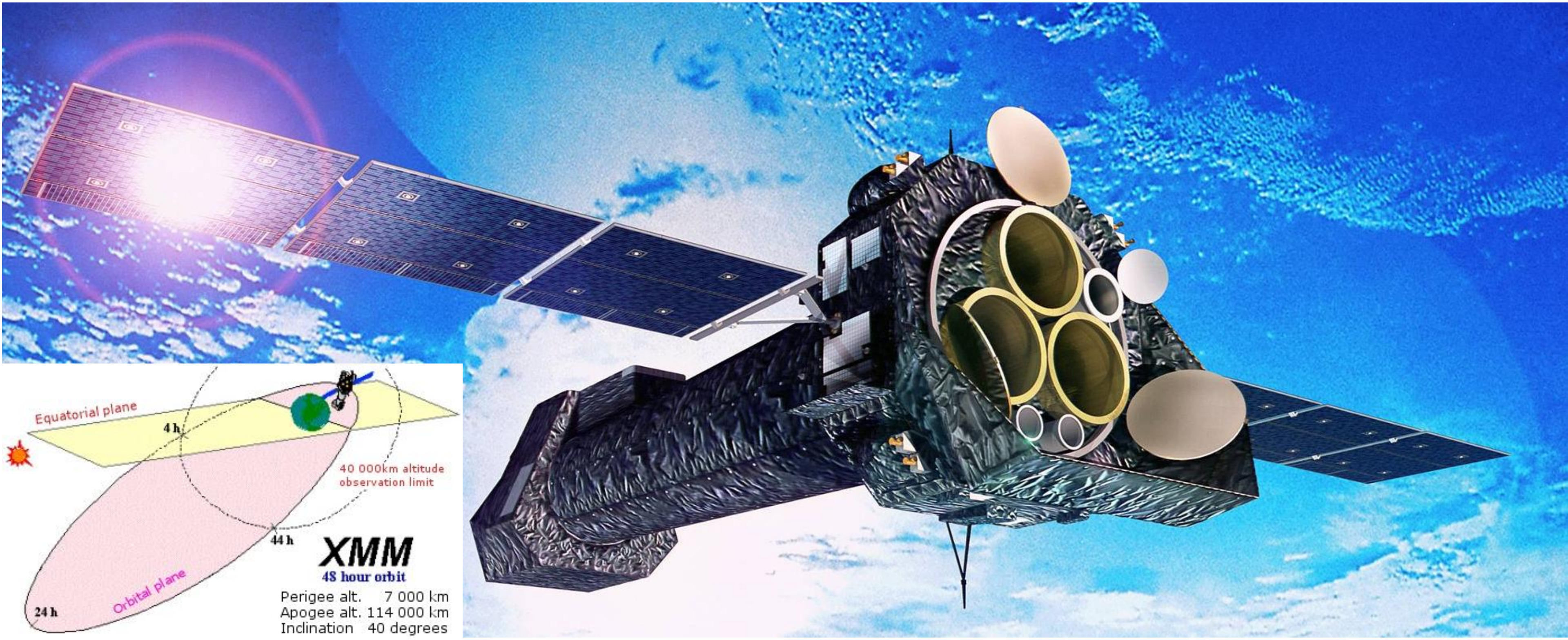

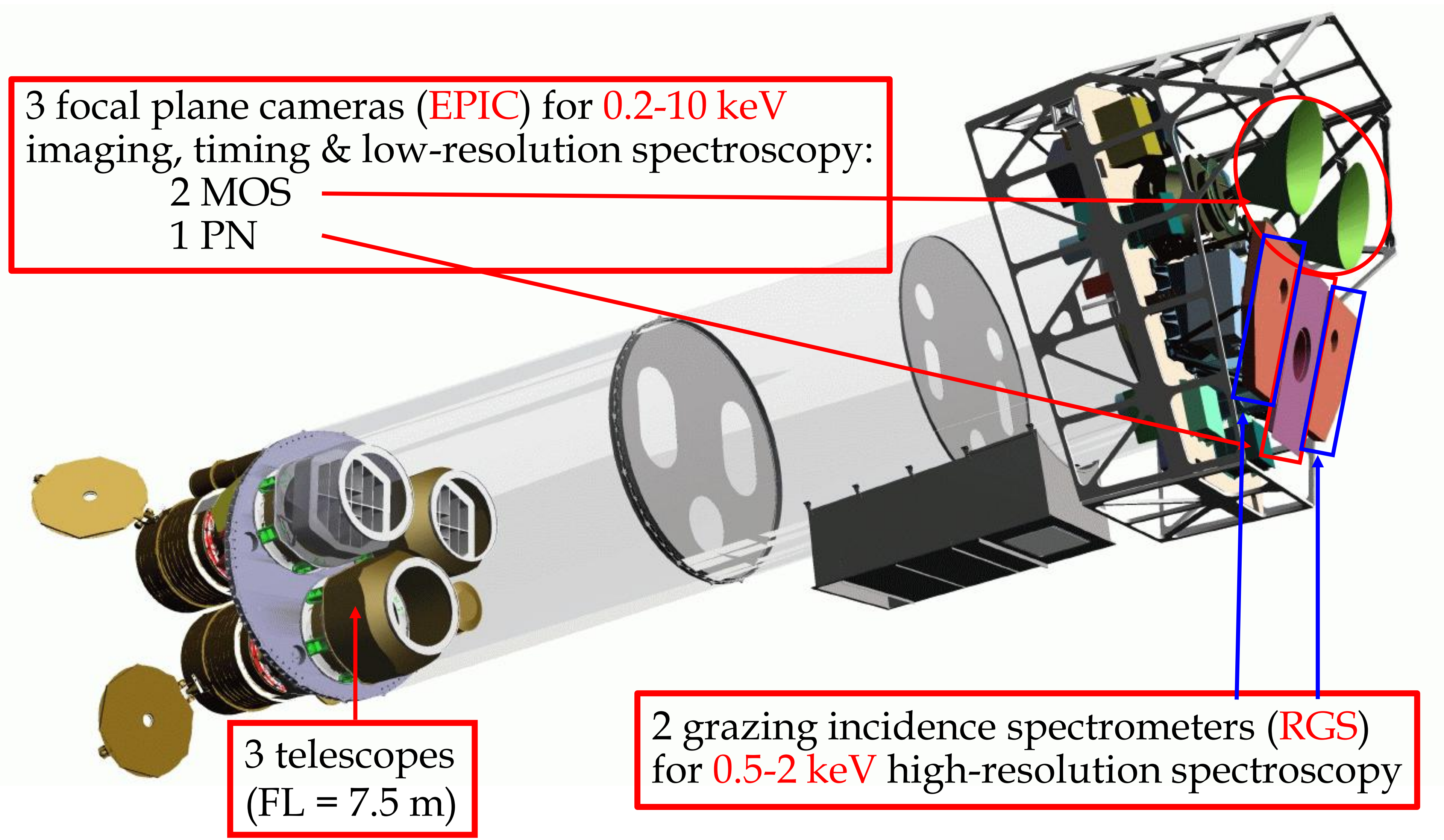
3 focal plane cameras (EPIC) for 0.2-10 keV imaging, timing & low-resolution spectroscopy:
2 MOS
1 PN
3 telescopes (FL = 7.5 m)
2 grazing incidence spectrometers (RGS) for 0.5-2 keV high-resolution spectroscopy

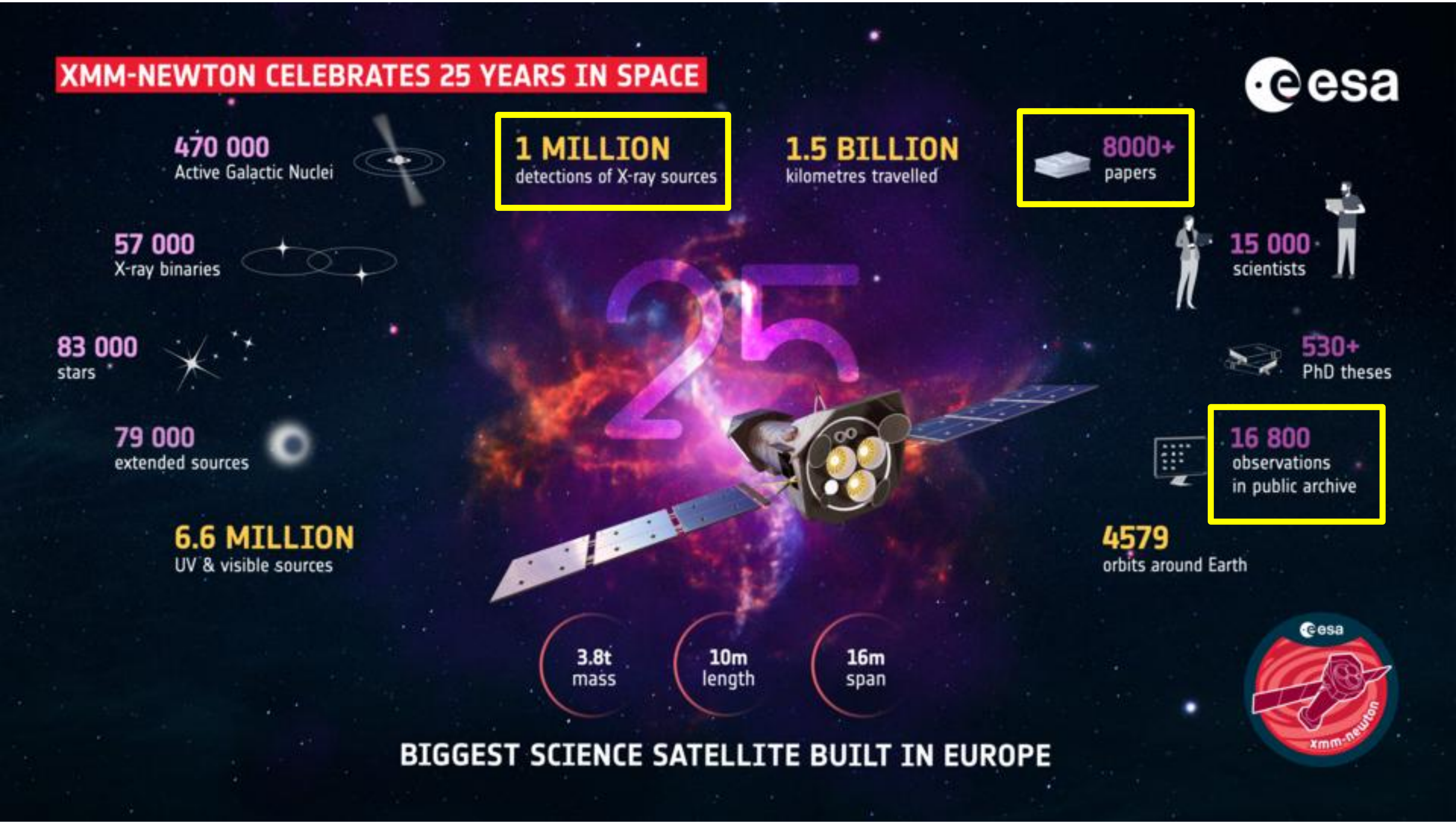

AO24: 12 Ms of observing time available, 86.3 requested ⇒ over-subscription factor 7.2

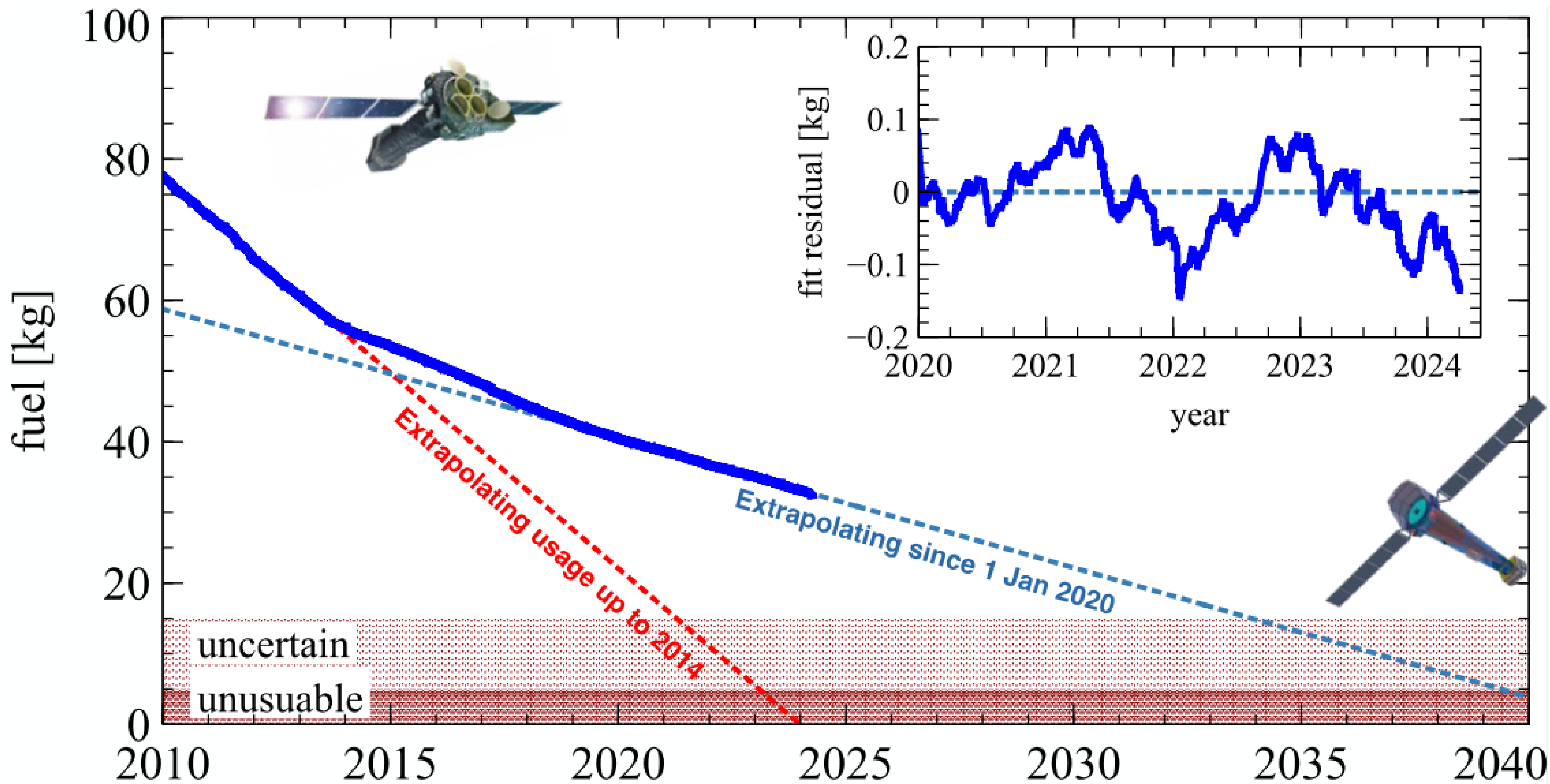

Operations extended until December 2026, and indicatively until end of 2029

We investigated with *XMM-Newton* the two extremes of the BeXRBs

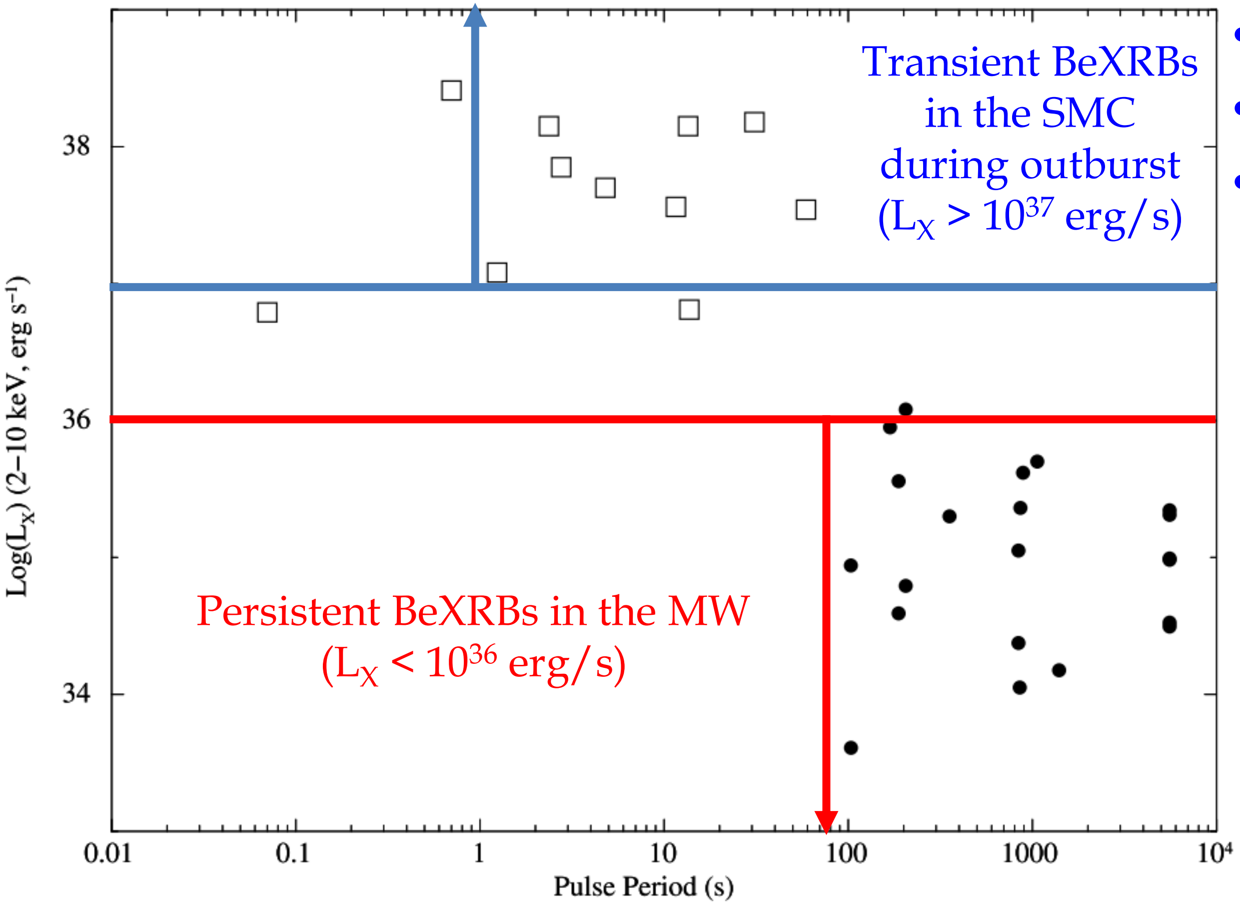

- Narrow orbits ($P_{orb} < 100$ d)
- High eccentricity
- Disk-fed accretion from high-density regions

- Wide orbits ($P_{orb} > 200$ d)
- High eccentricity
- Wind-fed accretion from low density regions

Persistent BeXRBs in the MW observed with *XMM-Newton*

X-ray source	P_{spin} (s)	L_X (2-10 keV, x10^{35} erg s^{-1})	Results in
X Persei	839.3	1.1	La Palombara & Mereghetti 2007
RX J0146.9+6121	1396.1	0.15	La Palombara & Mereghetti 2006
RX J1037.5-5647	853.4	0.11	La Palombara et al. 2009
RX J0440.9+4431	204.96	0.62	La Palombara et al. 2012
SXP 1062	1062	5.3	Hénault-Brunet et al. 2012
Swift J045106.8-694803	168.5	8.9	Bartlett, Coe, and Ho 2013
4U 0728-25	103.3	0.88	La Palombara et al. 2025

Persistent BeXRBs in the MW observed with *XMM-Newton*

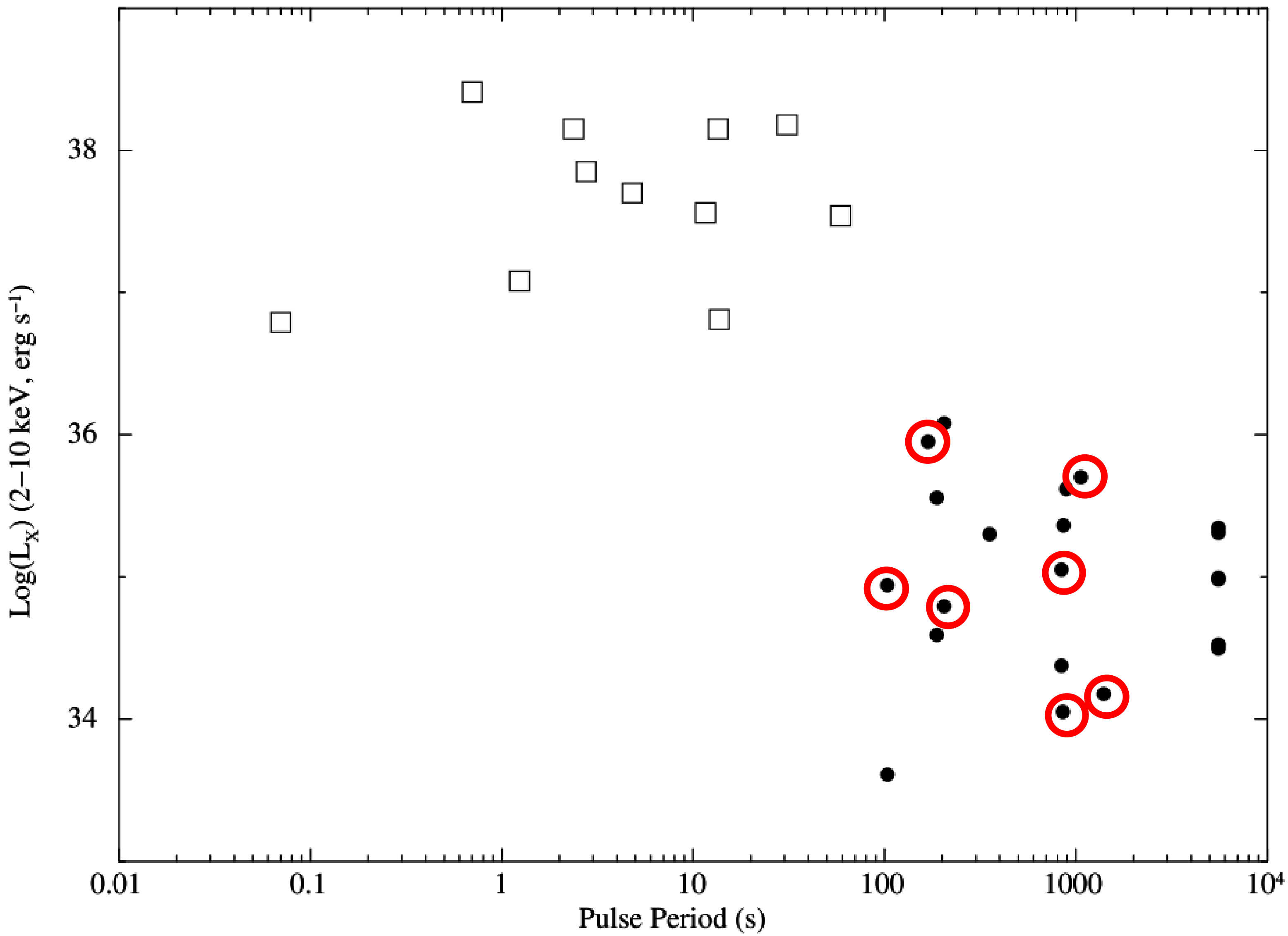

Timing analysis

Common properties:

- Broad single-peaked pulse profile
- Low energy dependence of the pulse profile

RX J0440.9+4431

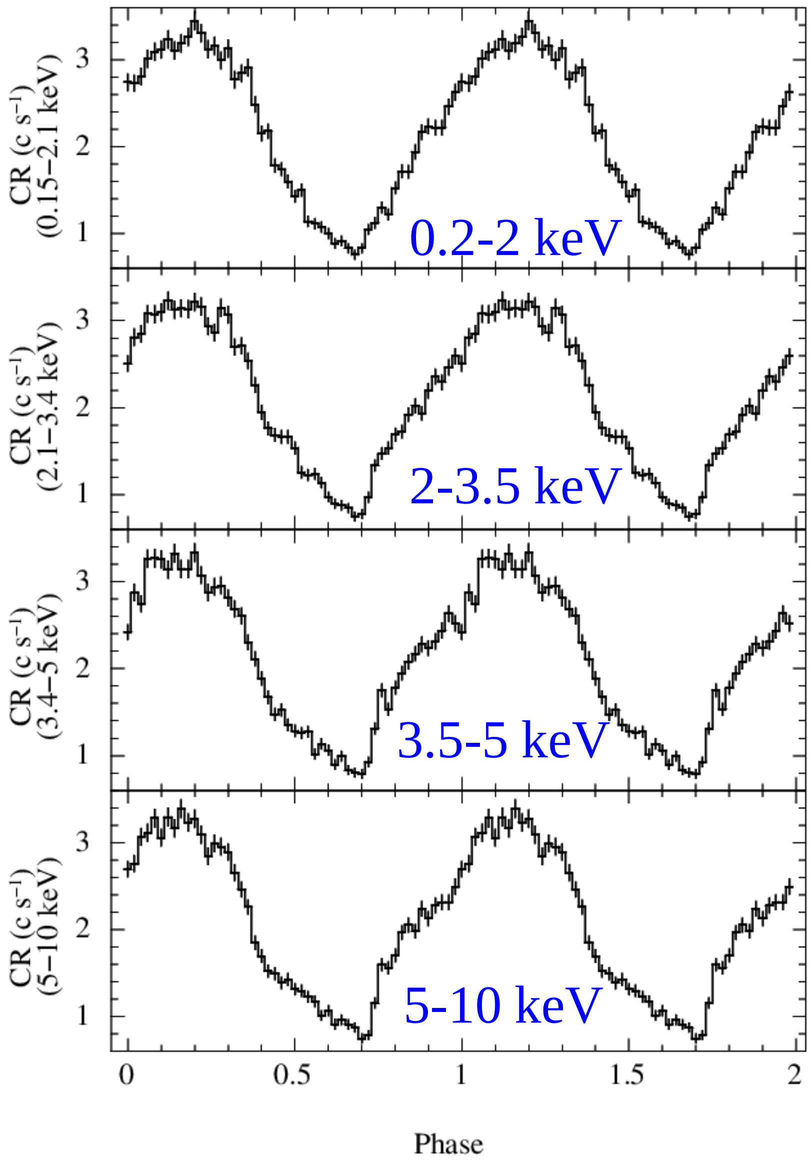

Spectral analysis

Common spectral properties:

- single component models (power law or blackbody)
  ⇒ **large residuals**
- alternative emission models
  ⇒ **rejected by data**
- power law + blackbody model
  ⇒ **good fit**
- no evidence of Iron line
  ⇒ **EQW Fe < 0.2 keV**

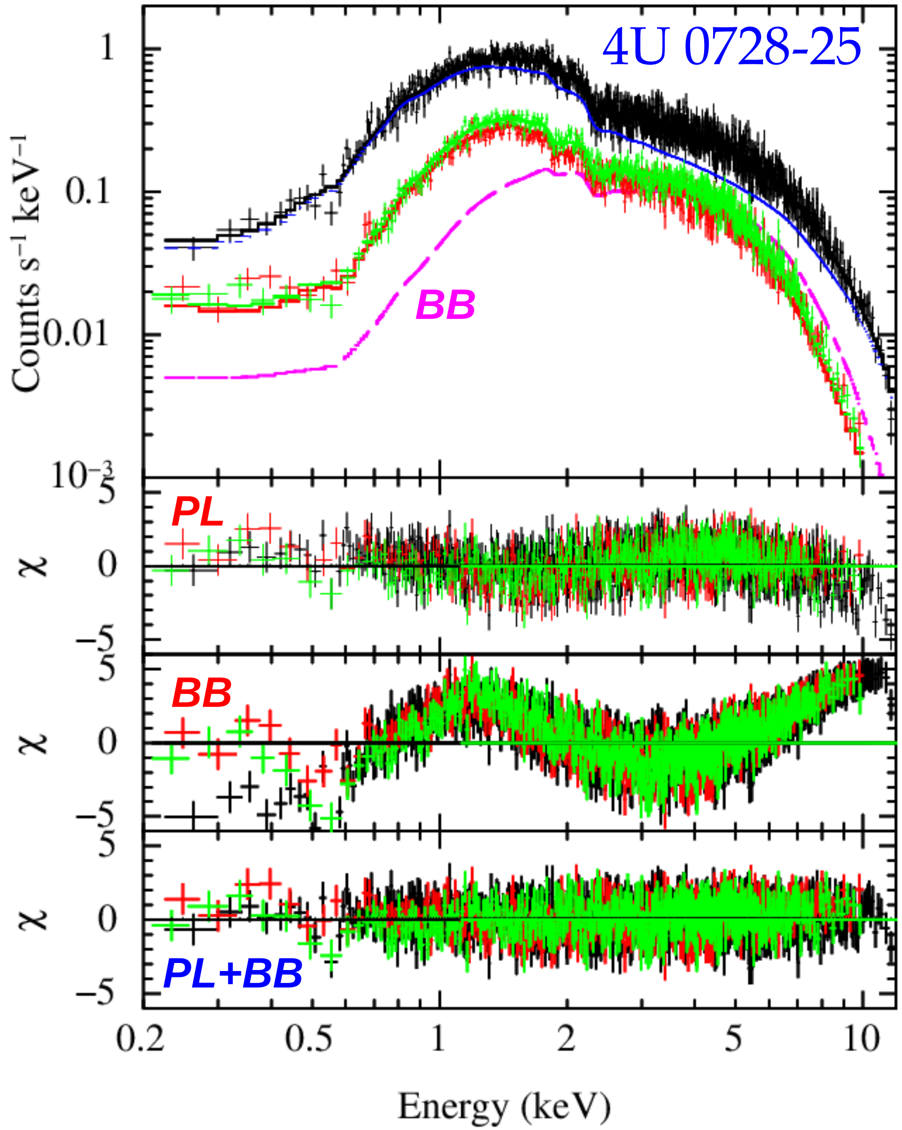

Spectral analysis

X-ray source	kT_{BB} (keV)
X Persei	1.42(+0.04/-0.02)
RX J0146.9+6121	1.11(+0.07/-0.06)
RX J1037.5-5647	1.26(+0.16/-0.09)
RX J0440.9+4431	1.34±0.04
SXP 1062	1.54±0.16
Swift J045106.8-694803	1.8(+0.2/-0.3)
4U 0728-25	1.52±0.06

- **high temperature** ($kT > 1$ keV)

Spectral analysis

X-ray source	kT_{BB} (keV)	R_{BB} (m)
X Persei	1.42(+0.04/-0.02)	361±3
RX J0146.9+6121	1.11(+0.07/-0.06)	140(+20/-10)
RX J1037.5-5647	1.26(+0.16/-0.09)	130(+10/-20)
RX J0440.9+4431	1.34±0.04	270±20
SXP 1062	1.54±0.16	490±50
Swift J045106.8-694803	1.8(+0.2/-0.3)	500±200
4U 0728-25	1.52±0.06	240(+30/-20)

- **high temperature** ($kT > 1$ keV)
- **small emission radius** ($R < 0.5$ km)

Spectral analysis

X-ray source	kT_{BB} (keV)	R_{BB} (m)	$flux_{BB}/flux_{TOT}$ (%)
X Persei	1.42(+0.04/-0.02)	361±3	39
RX J0146.9+6121	1.11(+0.07/-0.06)	140(+20/-10)	24
RX J1037.5-5647	1.26(+0.16/-0.09)	130(+10/-20)	42
RX J0440.9+4431	1.34±0.04	270±20	35
SXP 1062	1.54±0.16	490±50	21
Swift J045106.8-694803	1.8(+0.2/-0.3)	500±200	41
4U 0728-25	1.52±0.06	240(+30/-20)	24

- **high temperature** (kT > 1 keV)
- **small emission radius** (R < 0.5 km)
- **high BB contribution** (20-40 % of the total flux)

Spectral analysis

X-ray source	kT_{BB} (keV)	R_{BB} (m)	$flux_{BB}/flux_{TOT}$ (%)
X Persei	1.42(+0.04/-0.02)	361±3	39
RX J0146.9+6121	1.11(+0.07/-0.06)	140(+20/-10)	24
RX J1037.5-5647	1.26(+0.16/-0.09)	130(+10/-20)	42
RX J0440.9+4431	1.34±0.04	270±20	35
SXP 1062	1.54±0.16	490±50	21
Swift J045106.8-694803	1.8(+0.2/-0.3)	500±200	41
4U 0728-25	1.52±0.06	240(+30/-20)	24

- **high temperature** (kT > 1 keV)
- **small emission radius** (R < 0.5 km)
- **high BB contribution** (20-40 % of the total flux)

⇓

common property of persistent BeXRBs

Polar-cap origin of the BB component?

Assuming $M_{NS} = 1.4\ M_{SUN}$, $R_{NS} = 10^6$ cm and $B_{NS} = 10^{12}$ G, we can estimate:

- the accretion rate: $\dot{M} = LR_{NS}/(GM_{NS})$
- the magnetic dipole momentum: $\mu = B_{NS}R_{NS}^3/2$
- the magnetospheric radius: $R_m = \{\mu^4/[2GM\dot{M}^2]\}^{1/7}$
- the accretion column radius: $R_{col} \sim R_{NS}(R_{NS}/R_m)^{1/2}$

Polar-cap origin of the BB component?

X-ray source	kT_{BB} (keV)	R_{BB} (m)	$flux_{BB}/flux_{TOT}$ (%)	R_{col} (m)
X Persei	1.42(+0.04/-0.02)	361±3	39	330
RX J0146.9+6121	1.11(+0.07/-0.06)	140(+20/-10)	24	250
RX J1037.5-5647	1.26(+0.16/-0.09)	130(+10/-20)	42	240
RX J0440.9+4431	1.34±0.04	270±20	35	310
SXP 1062	1.54±0.16	490±50	21	420
Swift J045106.8-694803	1.8(+0.2/-0.3)	500±200	41	450
4U 0728-25	1.52±0.06	240(+30/-20)	24	340

Polar-cap origin of the BB component?

X-ray source	kT_{BB} (keV)	R_{BB} (m)	$flux_{BB}/flux_{TOT}$ (%)	R_{col} (m)
X Persei	1.42(+0.04/-0.02)	361±3	39	330
RX J0146.9+6121	1.11(+0.07/-0.06)	140(+20/-10)	24	250
RX J1037.5-5647	1.26(+0.16/-0.09)	130(+10/-20)	42	240
RX J0440.9+4431	1.34±0.04	270±20	35	310
SXP 1062	1.54±0.16	490±50	21	420
Swift J045106.8-694803	1.8(+0.2/-0.3)	500±200	41	450
4U 0728-25	1.52±0.06	240(+30/-20)	24	340

⇓

the observed thermal component is consistent with emission from the NS polar caps

Polar-cap origin of the BB component?

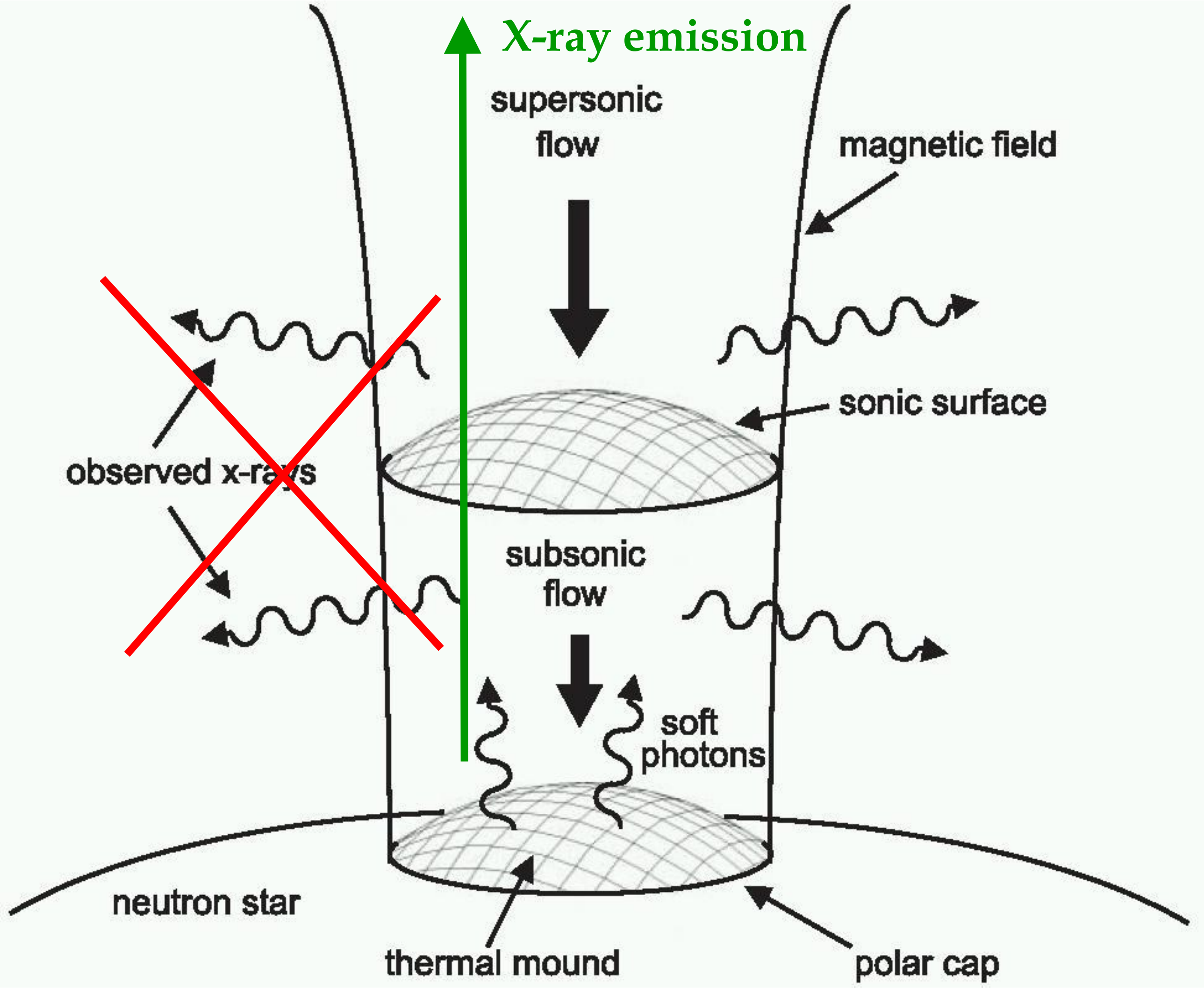

Becker & Wolff, 2007:
bulk and thermal Comptonization in a radiation dominated accretion column

BUT

low luminosity
($L_X < 10^{35}$ erg s^{-1})
⇓

- weak or absent shock
- BB component due to the thermal mound at the base of the accretion column
- pencil-beam emission rather than fan-beam

Transient BeXRBs in the SMC

Ideal site to investigate the *soft* spectral component at high luminosities:

- Several (> 100) sources
- $L_X \sim 10^{38}$ erg s^{-1} in outburst
- $N_H < 10^{21}$ cm^{-2}

} High count statistics at low energies

- Small uncertainties on the source distances ⇒ reliable estimate of L_X

Program of ToO observations with *XMM-Newton* performed between 2014 and 2017

⇓

4 sources observed in *outburst*:

X-ray source	P_{spin} (s)	L_X (0.2-10 keV, x10^{37} erg s^{-1})	Results in
RX J0059.2-7138	2.76	7	Sidoli et al. 2015
SMC X-2	2.37	14	La Palombara et al. 2016
IGR J01572-7259	11.58	3.6	La Palombara et al. 2018
SXP 59	58.95	3.5	La Palombara et al. 2018

Transient BeXRBs in the SMC

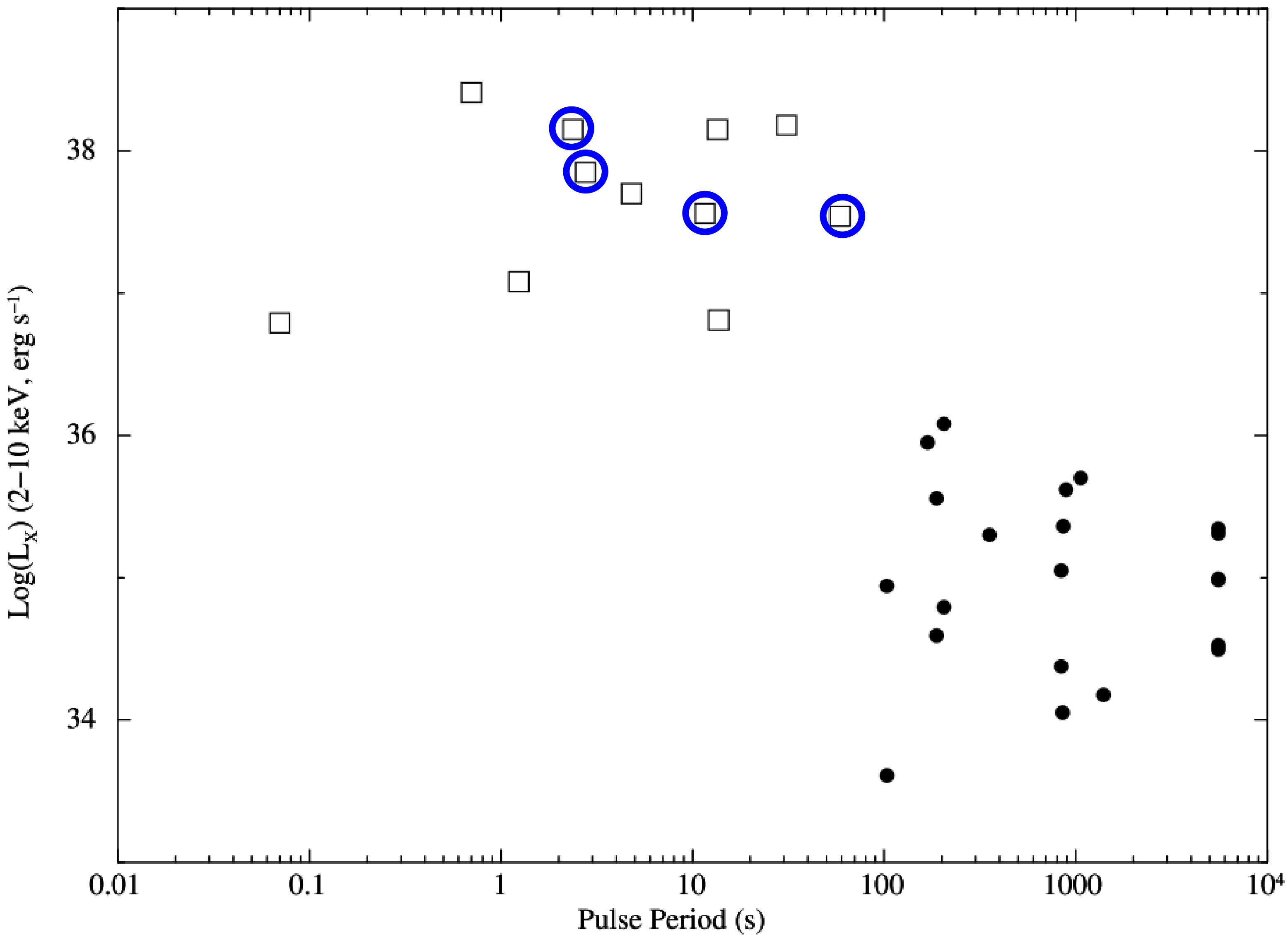

Timing analysis

Common properties:

- Pulsed emission also at low energies (E < 1 keV)
- Significant energy dependence of the pulse profile
- Double-peaked pulse profile at high energies
- Pulsed fraction increasing with E

SXP 59: *PF* < 30 % @ E < 1 keV, > 60 % @ E > 4.5 keV

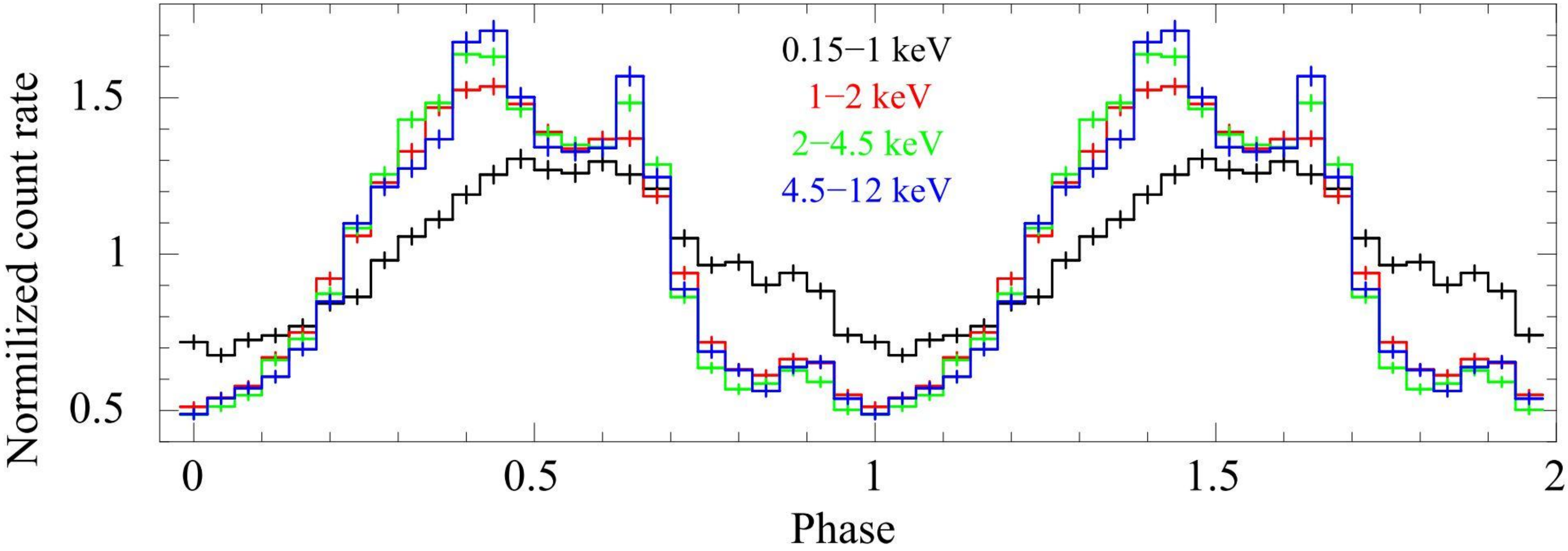

EPIC spectral analysis

SXP 59

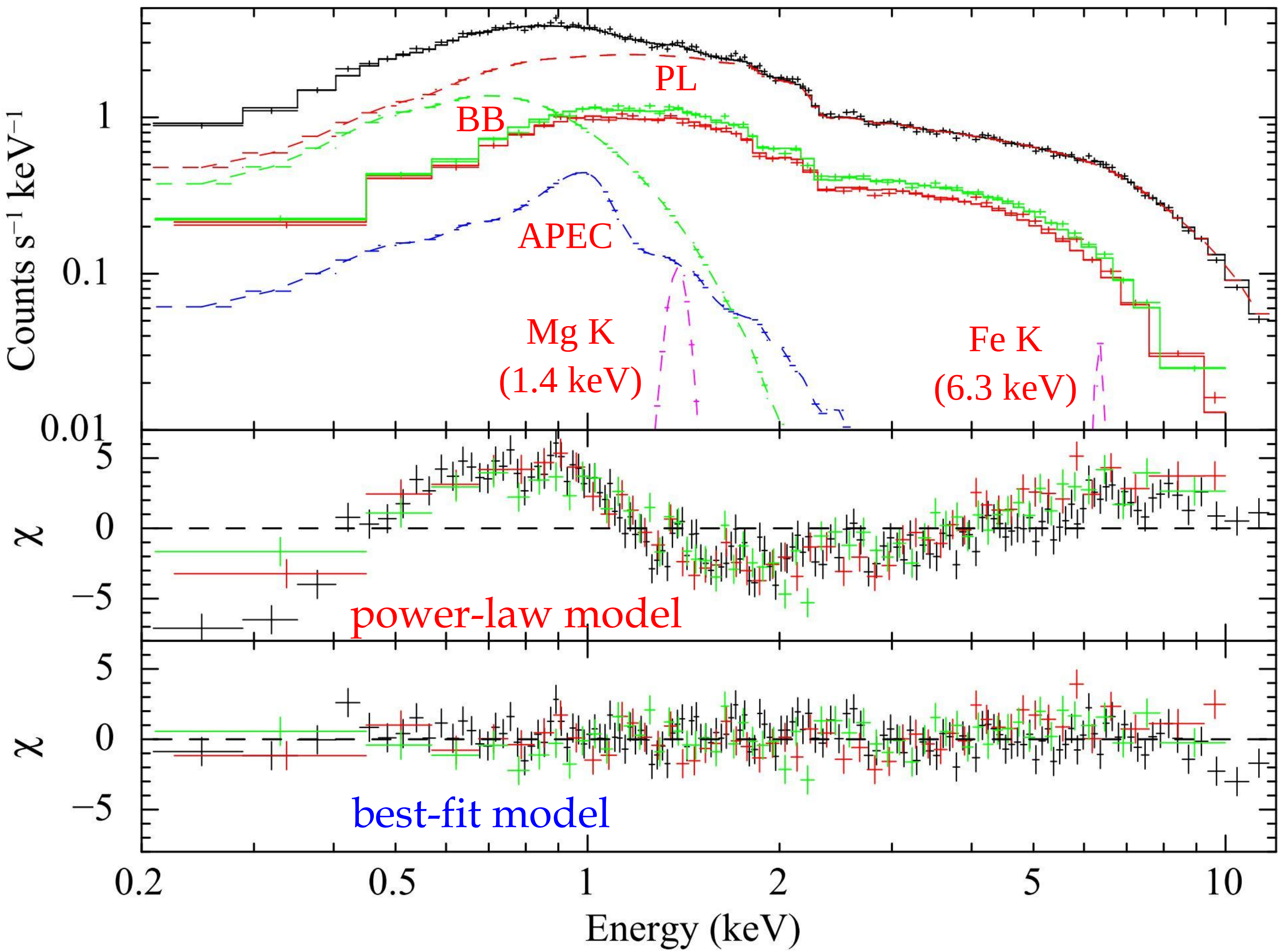

EPIC spectral analysis

X-ray source	kT_{BB} (eV)
RX J0059.2-7138	93±5
SMC X-2	130(+20/-10)
IGR J01572-7259	220(+10/-20)
SXP 59	170±10

- **low temperature** (kT < 0.2 keV)

EPIC spectral analysis

X-ray source	kT_{BB} (eV)	R_{BB} (km)
RX J0059.2-7138	93±5	350(+80/-50)
SMC X-2	130(+20/-10)	320(+120/-90)
IGR J01572-7259	220(+10/-20)	50(+6/-5)
SXP 59	170±10	110(+20/-10)

- **low temperature** (kT < 0.2 keV)
- **large emission radius** (R > 50 km)

EPIC spectral analysis

X-ray source	kT_{BB} (eV)	R_{BB} (km)	$flux_{BB}/flux_{TOT}$ (%)
RX J0059.2-7138	93±5	350(+80/-50)	1.7
SMC X-2	130(+20/-10)	320(+120/-90)	3.1
IGR J01572-7259	220(+10/-20)	50(+6/-5)	1.6
SXP 59	170±10	110(+20/-10)	3.5

- **low temperature** (kT < 0.2 keV)
- **large emission radius** (R > 50 km)
- **low BB contribution** (< 4 % of the total flux)

EPIC spectral analysis

X-ray source	kT_{BB} (eV)	R_{BB} (km)	$flux_{BB}/flux_{TOT}$ (%)
RX J0059.2-7138	93±5	350(+80/-50)	1.7
SMC X-2	130(+20/-10)	320(+120/-90)	3.1
IGR J01572-7259	220(+10/-20)	50(+6/-5)	1.6
SXP 59	170±10	110(+20/-10)	3.5

- **low temperature** (kT < 0.2 keV)
- **large emission radius** (R > 50 km)
- **low BB contribution** (< 4 % of the total flux)

⇓

common property of transient BeXRBs in ouburst

Common properties of transient BeXRBs in outburst

- High luminosity: $L_X = 10^{37\text{-}38}$ erg s^{-1}
- High pulsed fraction: $PF > 30$ %, increasing with energy
- Double-peaked pulse profile ⇒ fan-beam emission geometry?
- *Soft excess* which:
  - ✓ is faint: $L_{SE}/L_{PL} = 2\text{-}3$ %
  - ✓ pulsates (from phase-resolved spectral analysis)
  - ✓ is dominated by a cold ($kT_{BB} \sim 0.1\text{-}0.2$ keV) but large ($R_{BB} \sim 100$ km) BB emission
  - ✓ d_{BB} (BB distance from central NS) ~ R_m (magnetospheric radius)

⇓

reprocessing of the primary emission
by the optically thick material at the
inner edge of the accretion disc

Common properties of transient BeXRBs in outburst

- High luminosity: $L_X = 10^{37-38}$ erg s^{-1}
- High pulsed fraction: *PF* > 30 %, increasing with energy
- Double-peaked pulse profile ⇒ fan-beam emission geometry?
- *Soft excess* which:
  - ✓ is faint: L_{SE}/L_{PL} = 2-3 %
  - ✓ pulsates (from phase-resolved spectral analysis)
  - ✓ is dominated by a cold (kT_{BB} ~ 0.1-0.2 keV) but large (R_{BB} ~ 100 km) BB emission
  - ✓ d_{BB} (BB distance from central NS) ~ R_m (magnetospheric radius)

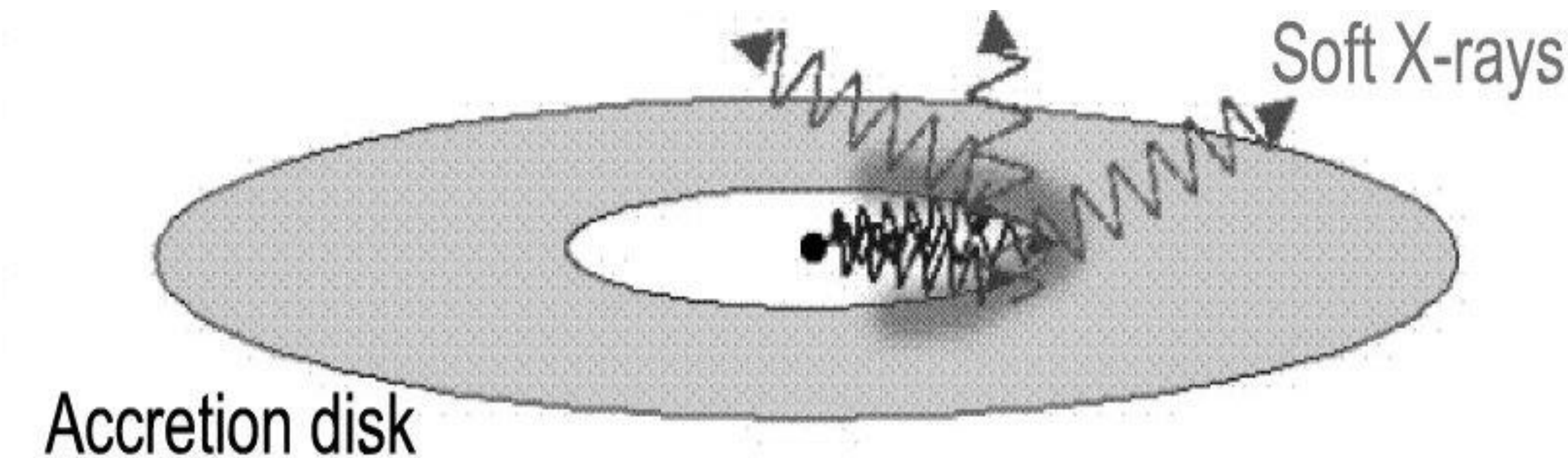

RGS spectral analysis

first detection of several emission lines due to N, O, Ne, Mg, Si, and Fe

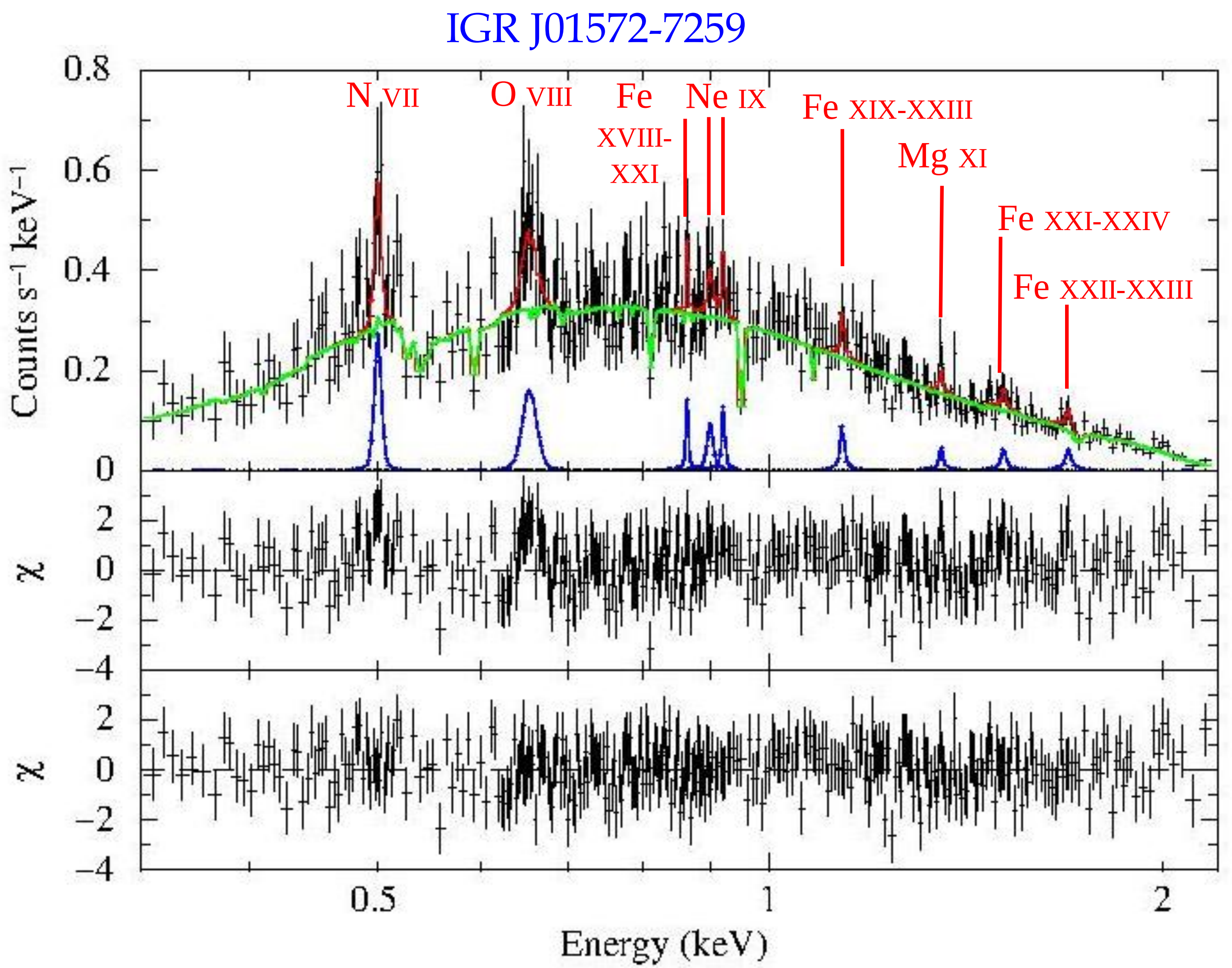

Common properties of transient BeXRBs in outburst

- High luminosity: $L_X = 10^{37\text{-}38}$ erg s^{-1}
- High pulsed fraction: *PF* > 30 %, increasing with energy
- Double-peaked pulse profile ⇒ fan-beam emission geometry?
- *Soft excess* which:
  - ✓ includes narrow lines due to emission from photoionized plasma in regions above the disc

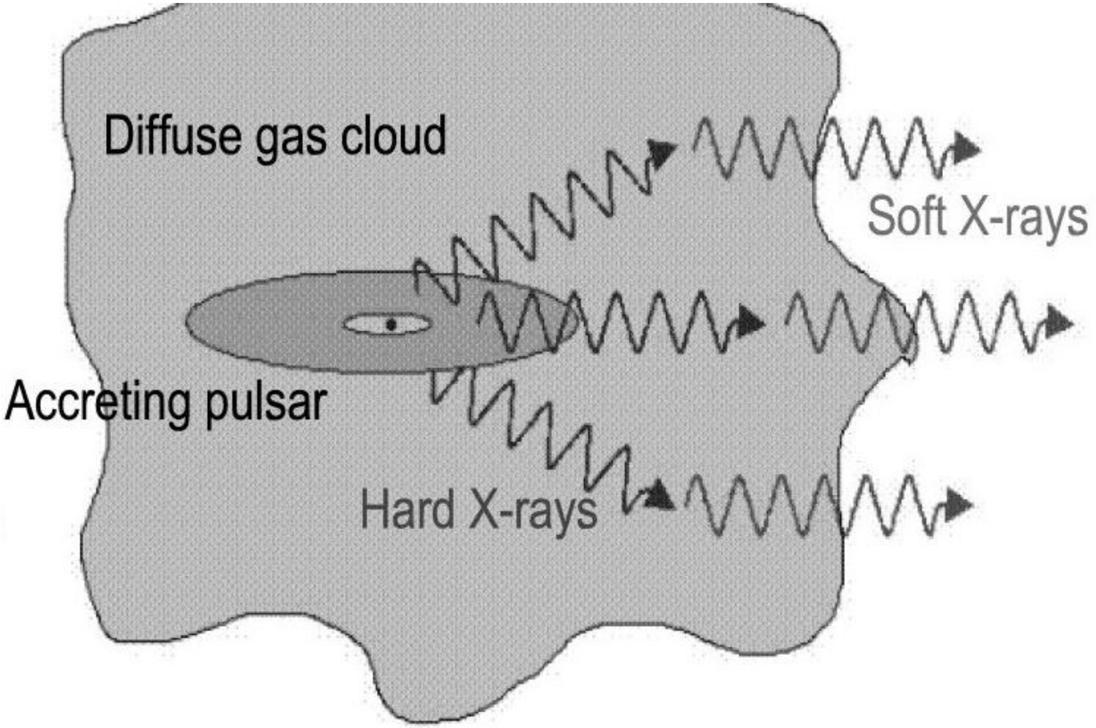

Conclusions

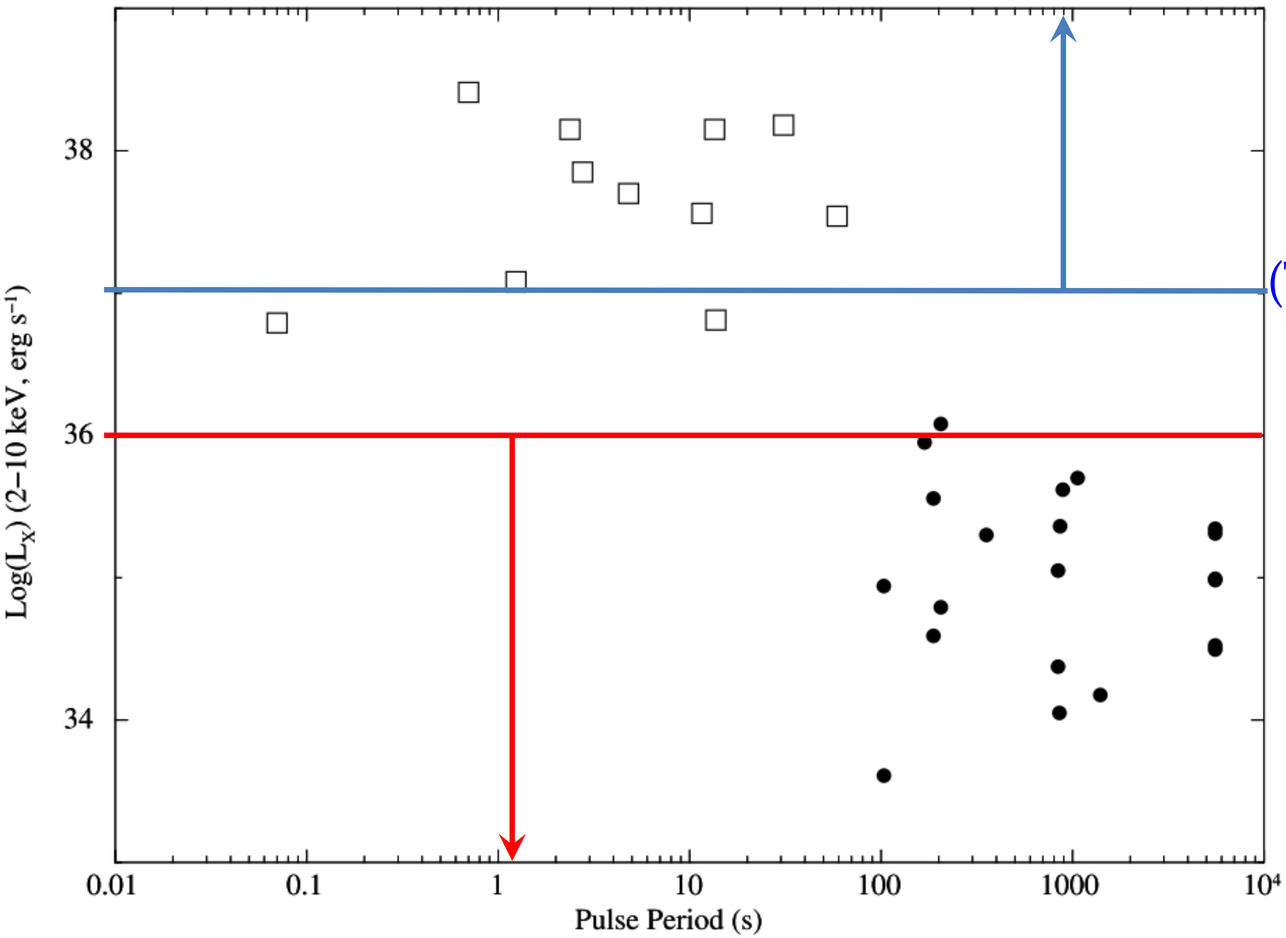

$L_X \geq 10^{37}$ erg s^{-1}

⇓

Soft Excess

(cold BB + narrow lines)

(T_{BB} < 0.5 keV & R_{BB} > 100 km)

$L_X \leq 10^{36}$ erg s^{-1}

⇓

mainly *hot-bb excess*

(T_{BB} > 1 keV & R_{BB} < 0.5 km)

⇓

- **a <u>hot-BB excess</u> is a common feature of the <u>low-L & long-P</u> binary pulsars**
- **a <u>soft excess</u> is a common feature of the <u>high-L & short-P</u> binary pulsars**

Thanks for your attention!

Back-up slides

P_{spin}-P_{orb} period ("Corbet diagram")

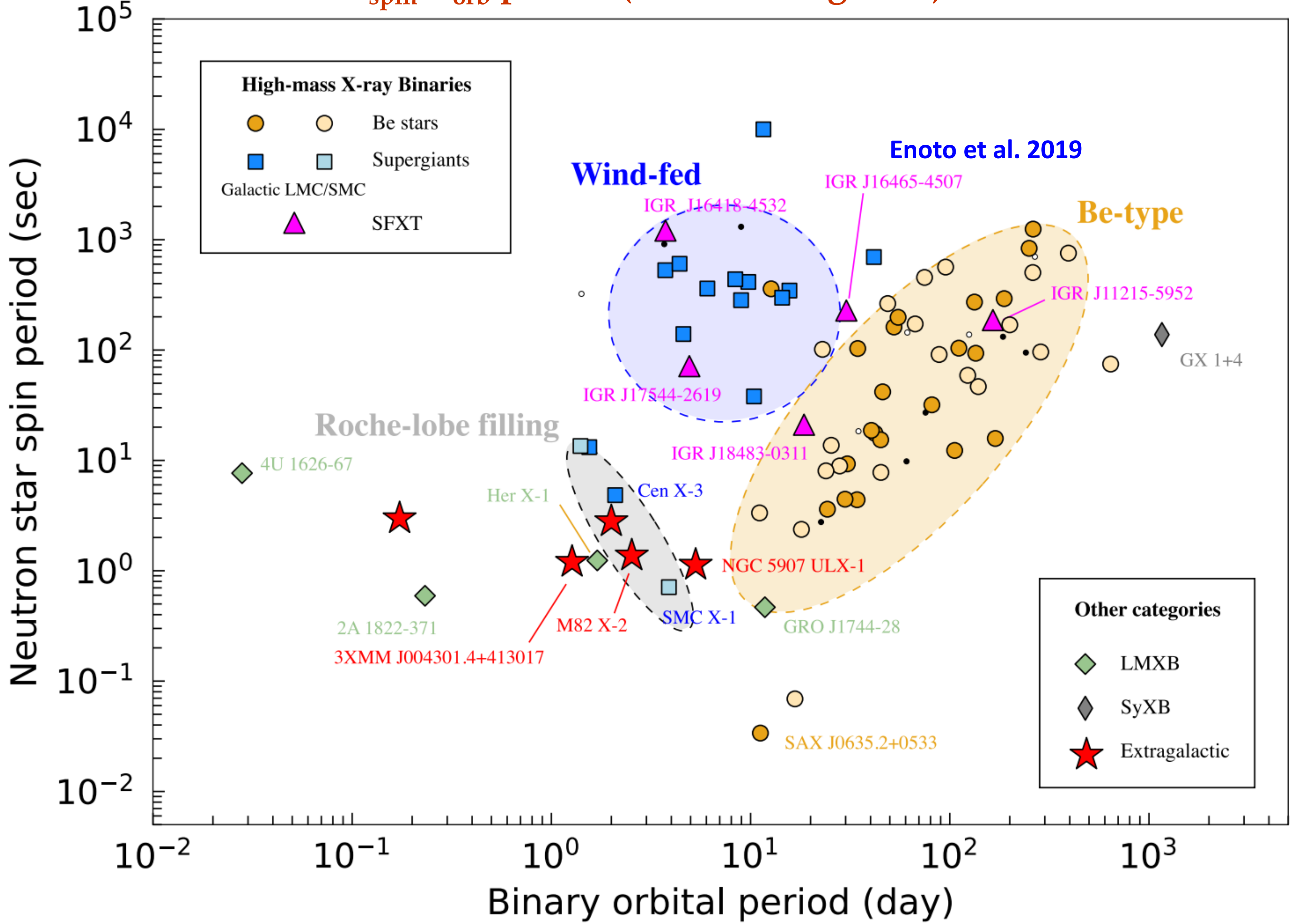

Be binaries detected at VHE

Name	Star spectral type	P_{spin} (ms)	P_{orb}
PSR B1259-63	O9.5 Ve	48	1236.72 days
PSR J2032+4127	B0 Ve	143	50 years
LS I +61° 303	B0 Ve	270	26.49 days
HESS J0632+057	B0e	-	315.5 days

Be binaries detected at VHE

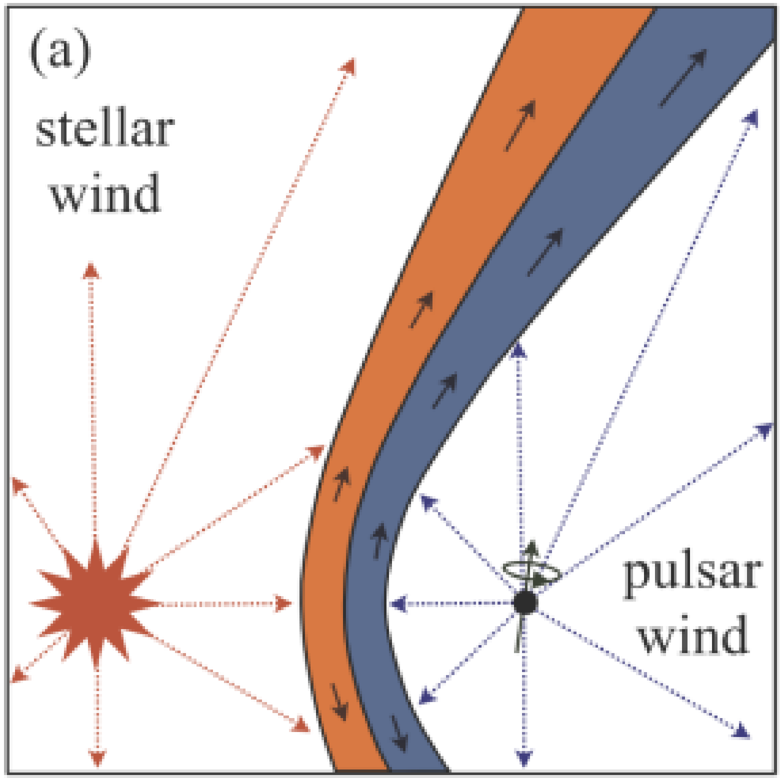

X Persei

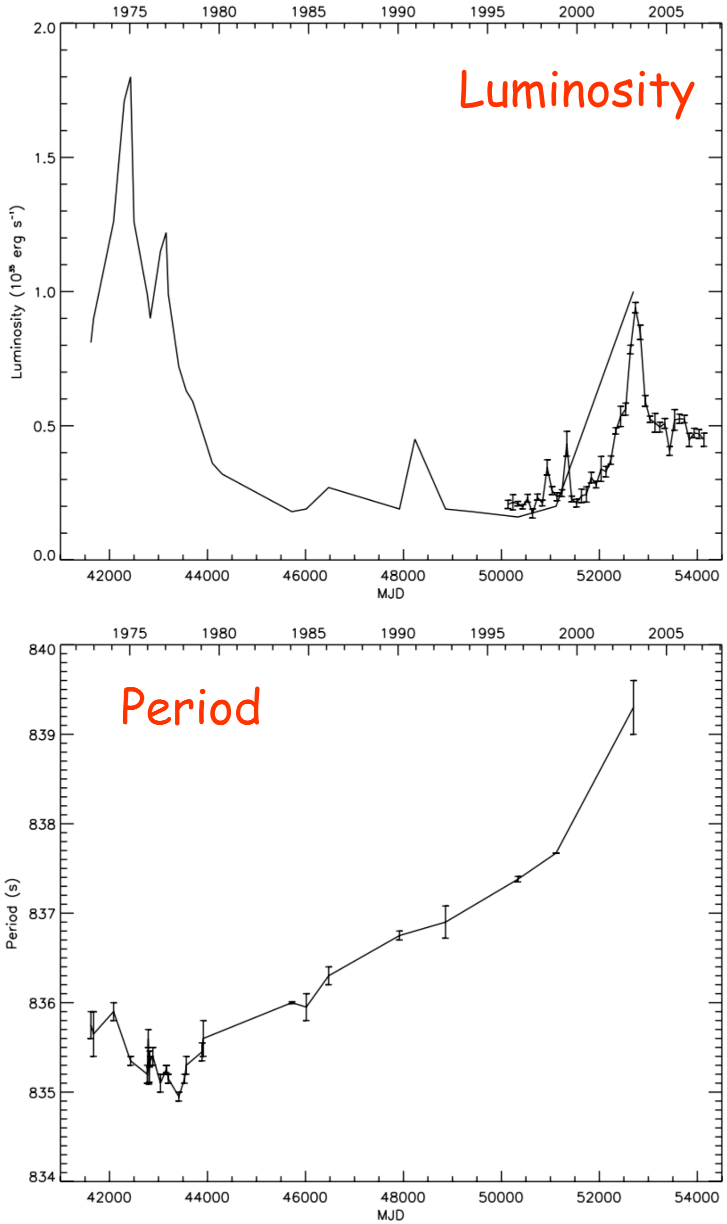

RX J0146.9+6121

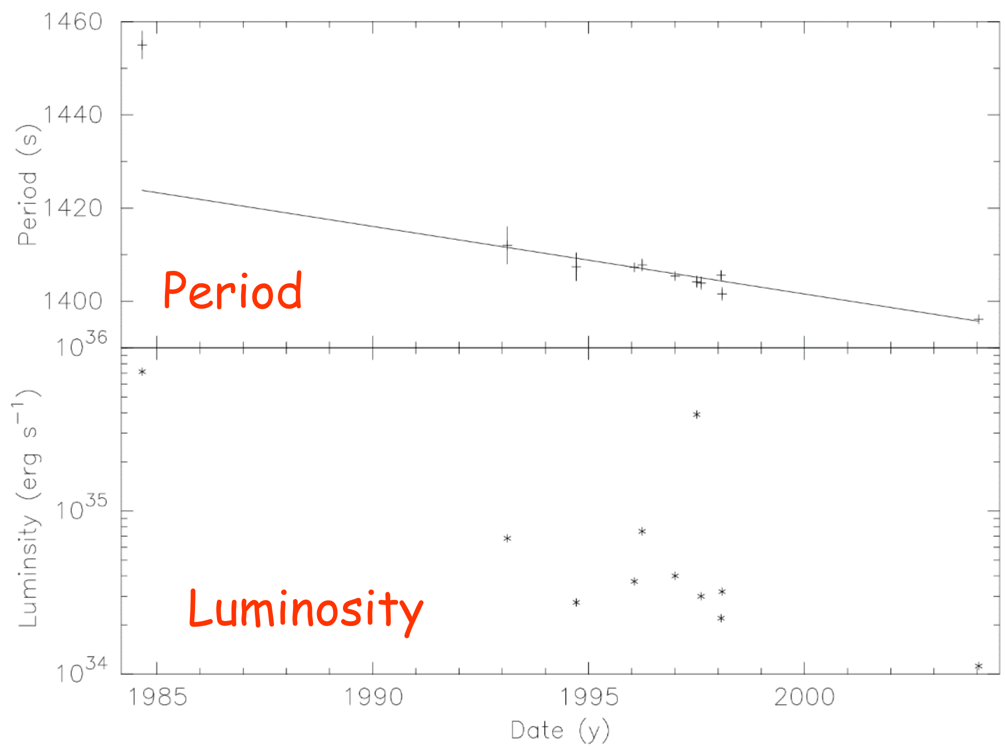

SXP59.0: long-term evolution

Luminosity variability of more than 3 orders of magnitude

P_{spin} variation of ~ 0.3 s

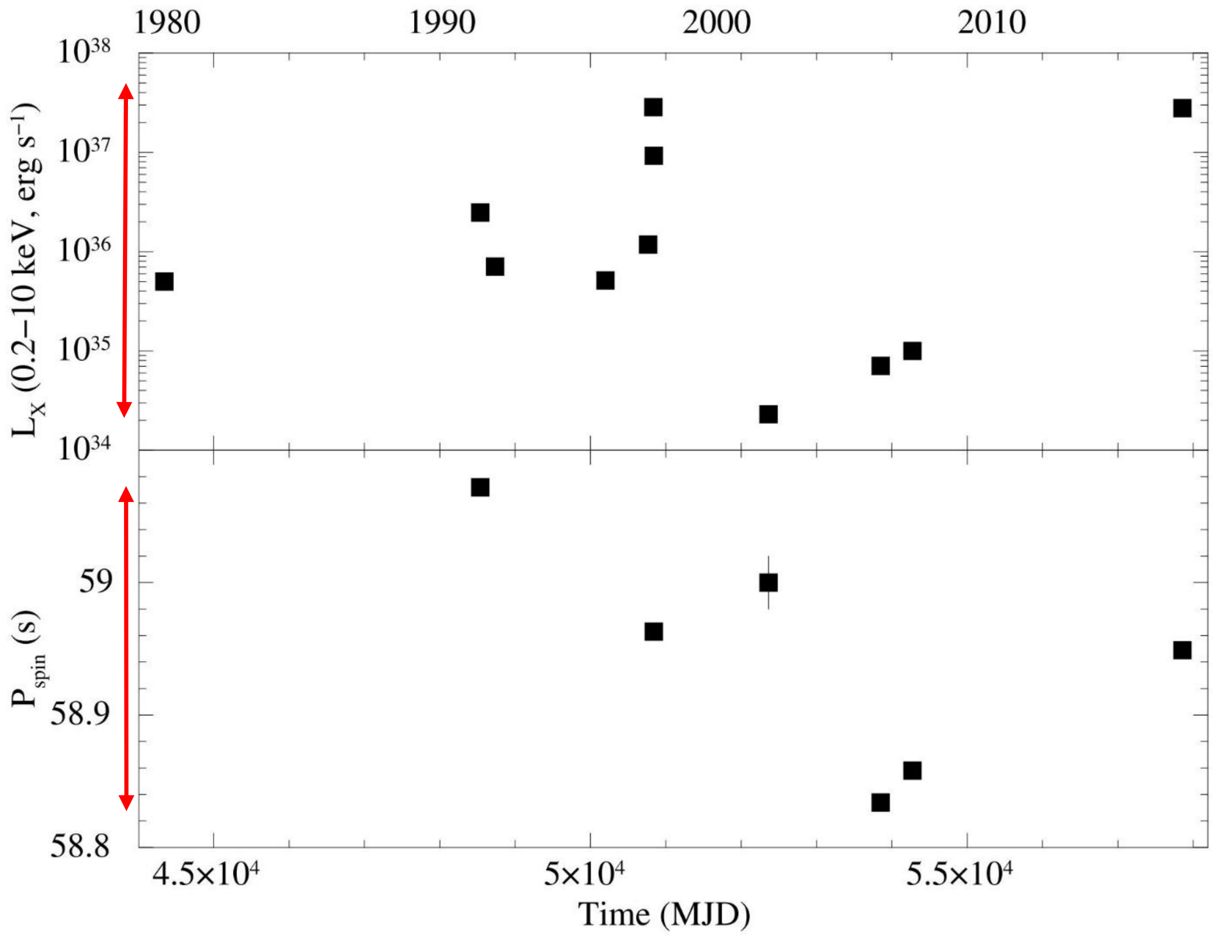

P_{spin} variation due to NS orbit ≅ 0.02 s

⇒ variability due to the pulsar spin-up and spin-down during the outburst and quiescence phases